ACS APPLIED MATERIALS & INTERFACES

Research Article

www.acsami.org

Green Synthesis of Bifunctional Fluorescent Carbon Dots from Garlic for Cellular Imaging and Free Radical Scavenging

Shaojing Zhao,[†,‡] Minhuan Lan,[†,‡] Xiaoyue Zhu,[‡] Hongtao Xue,[‡] Tsz-Wai Ng,[‡] Xiangmin Meng,[*,§] Chun-Sing Lee,[‡] Pengfei Wang,[§] and Wenjun Zhang[*,‡]

[‡]Center of Super-Diamond and Advanced Films (COSDAF) and Department of Physics and Materials Science, City University of Hong Kong, Hong Kong SAR, P.R. China

[§]Key Laboratory of Photochemical Conversion and Optoelectronic Materials, Technical Institute of Physics and Chemistry, Chinese Academy of Sciences, Beijing 100190, P.R. China

Supporting Information

ABSTRACT: Nitrogen and sulfur codoped carbon dots (CDs) were prepared from garlic by a hydrothermal method. The as-prepared CDs possess good water dispersibility, strong blue fluorescence emission with a fluorescent quantum yield of 17.5%, and excellent photo and pH stabilities. It is also demonstrated that the fluorescence of CDs are resistant to the interference of metal ions, biomolecules, and high ionic strength environments. Combining with low cytotoxicity properties, CDs could be used as an excellent fluorescent probe for cellular multicolor imaging. Moreover, the CDs were also demonstrated to exhibit favorable radical scavenging activity.

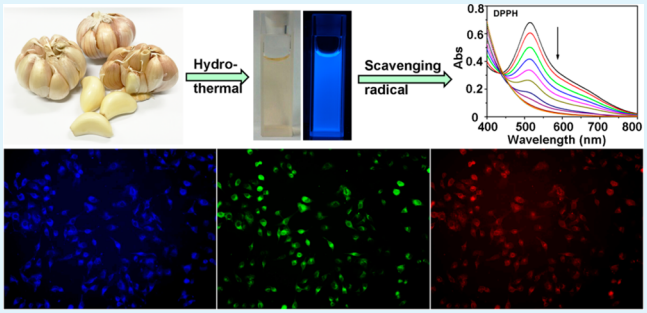

KEYWORDS: *carbon dots, fluorescence, reactive oxygen species, radical scavenging activity, multicolor imaging*

1. INTRODUCTION

As a new member of carbon nanomaterials, carbon dots (CDs) or carbon nanoparticles (CNPs) have a unique combination of the major outstanding properties of semiconductor quantum dots (QDs) but without incurring the burden of intrinsic toxicity. The excellent chemical and photochemical stability of CDs together with their biocompatibility give a clear advantage in the context of biological applications, and thus making them a legitimate competitor to the conventional QDs with comparable or even better performance.[1−5] Moreover, the surface of CDs can be readily modified with different functional groups, which enables more prospects for tuning their physicochemical properties.[6,7] Since the discovery of fluorescent CDs during the separation and purification of single-walled carbon nanotubes by Xu et al.,[8] a variety of approaches for synthesizing CDs have been developed, e.g., electrochemical synthesis, acidic oxidation, solvothermal, arc discharge, laser ablation, and oxygen plasma treatment.[9−12] Among them, solvothermal methods using cheap and eco-friendly biomass such as green tea, sweet potatoes, honey, bamboo leaves, and pomelo peel as the carbon sources to produce CDs have induced great interest because of their green chemistry nature.[13−17] The approach is also more cost-effective as compared to those applied for synthesizing other fluorescence nanoparticles, such as noble metal nanoparticles and semiconductor QDs.

One of the most fascinating characteristics of CDs is their photoluminescent capability. Although the exact mechanism of photoluminescence from CDs has not been fully understood,[18] the successful applications of CDs as a desirable fluorescent probe to visualize biological systems both in vitro and in vivo have been demonstrated, and following the work by Sun et al.,[19] the bioimaging capabilities of CDs have been extensively studied.[20−23] In addition, CDs have been found some other applications in the fields of chemical sensing, photocatalysis and phototherapy.[24−31] For instance, Markovic et al. found that electrochemically produced CDs could generate reactive oxygen species (ROS) including $^1O_2$ and $OH^•$ upon exposure to blue light and thus were applied to kill cancer cells and bacteria by causing oxidative stress.[32,33] Juzenas et al. also reported that CDs with a poly(propionyl ethylenimine-*co*-ethylenimine) coating could activate and generate $O_2^{•−}$ under UV irradiation. Although the ROS quantum yield was not reported, the human prostate adenocarcinoma (Du145 and PC3) cells were shown to be more sensitive to UV irradiation when preincubated with these CDs, and a decrease of cell viability by 20−30% was observed.[34]

Recently, we have prepared N, S-dual doped red fluorescent graphene QDs (one type of CDs) by using a N- and S-

Received: April 14, 2015
Accepted: July 20, 2015
Published: July 20, 2015

DOI: 10.1021/acsami.5b03228
ACS Appl. Mater. Interfaces 2015, 7, 17054−17060

containing polymer as the precursor. The graphene QDs could produce $^1O_2$ under visible light irradiation via a multistate sensitization process, resulting in a quantum yield of ~130%, and they were thus successfully applied in in vitro and in vivo photodynamic therapy.[35] Moreover, using trisodium citrate as the carbon source and melamine as the nitrogen source, we also prepared blue fluorescent N-doped CNPs by microwave-assisted hydrothermal method. However, neither ROS generation nor photothermal effects were observed in these N-doped CNPs.[36,37] These results suggest that the synthesis routes, reaction precursors, and dopants in CDs may strongly affect the photophysical and photochemical properties of the CDs.

In this work, we report the preparation of fluorescent N, S-*co*-doped CDs by a facile, green, and low-cost hydrothermal method using garlic as the precursor. The microstructure and chemical composition of the CDs were analyzed, and the cytotoxicity, stability, and fluorescence properties of the CDs were investigated in details. The application of the CDs in cellular multicolor imaging was demonstrated. Moreover, we also revealed that, different from most of the previous reported CDs, the as-prepared CDs exhibit excellent radical scavenging activity (RSA), which further expands their biological applications.

2. EXPERIMENTAL SECTION

2.1. Materials. NaCl, $Mn(CH_3COO)_2$-$4H_2O$, KCl, $Co(CH_3COO)_2$, $Al(NO_3)_3$-$9H_2O$, $Ni(CH_3COO)_2$, $Cu(CH_3COO)_2$-H_2O, $FeCl_3$, $CeCl_3$-$7H_2O$, $Cs(CH_3COO)_2$-H_2O, $LiNO_3$, $Ba(CH_3COO)_2$, $CdSO_4$, $MgCl_2$-$6H_2O$, $HgCl_2$, $FeCl_2$, 4-(2-Hydroxyethyl)piperazine-1-ethanesulfonic acid (HEPES), H_2O_2, RNA, DNA, cysteine (Cys), serine (Ser), homocysteine (Hcy), leucine (Leu), glutathione (GSH), valine (Val), aspartic acid (Asp), tyrosine (Tyr), tryptophan (Trp), alanine (Ala), methionine (Met), threonine (Thr), glycine (Gly), isoleucine (Ile), argine (Arg), lysine (Lys), quercetin (99%), fluorescein isothiocyanate (FITC), 3-(4,5-dimethylthiazol-2-yl)-2,5-diphenyltetrazolium bromide (MTT), salicylic acid, 1,1-diphenyl-2-picrylhydrazyl (DPPH), and ascorbic acid were purchased from Sigma-Aldrich Co. LLC. All chemicals were directly used without further purification. Deionized water with conductivity of 18.2 MΩ cm^{-1} used in this experiment was purified by the Millipore water purification system. White garlic as shown in Scheme 1 was used as the reaction precursor.

Scheme 1. Illustration of the Formation Process of Carbon Dots from Garlic by Hydrothermal Treatment

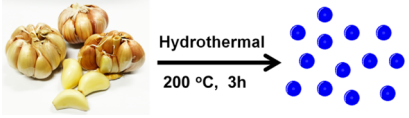

2.2. Preparation of CDs. CDs were synthesized through hydrothermal treatment of garlic, as demonstrated in Scheme 1. In detail, 0.5 g of garlic cloves and 15 mL of H_2O were added into an autoclave and heated at 200 °C for 3 h. After cooling to room temperature, large particles in the solution were removed through centrifugation and filtering. The CDs were further purified by dialyzing and then stored at 4 °C.

2.3. Characterization of CDs. The absorption and fluorescence spectra of the CDs were recorded on Shimadzu 1700 spectrophotometer and Hitachi FL 4600 fluorescence spectrophotometer at room temperature, respectively. X-ray photoelectron spectroscopy (XPS) measurements were carried out on a VG ESCALAB 220i-XL surface analysis system. Fourier transform infrared spectroscopy (FTIR) was performed on an IFS 66 V/S (Bruker) spectrometer. X-ray diffraction (XRD) patterns were obtained using an X-ray diffractometer (Bruker, D2 PHASER). Elemental analysis of CDs was carried out by using the FLASH EA1112 elemental analyzer. Transmission electron microscopy (TEM) images were acquired by using a Philips CM200 electron microscope. Quinine sulfate was used as the standard substance (0.1 M H_2SO_4 aqueous solution, fluorescent quantum yield ~ 54%) to measure the fluorescent quantum yield of CDs.[38] The pH value of the solution was measured by the pH-meter (Eutech PH 700).

2.4. Cellular Imaging and MTT Assay. A549 cells were obtained from the ATCC. The cell culture medium is DMEM/F12 containing 50 unit/mL penicillin, 50 μg/mL of streptomycin and 10% fetal bovine serum (FBS). For in vitro cellular imaging studies, A549 cells were seeded in a 6-well plate with the density of 10^4 cells per well and incubated for 24 h in a humidified incubator containing 5% CO_2 at 37 °C. The cells were then incubated with fresh culture medium containing 100 μL of CDs aqueous solution for 4 h. Finally, the cells were washed by phosphate-buffered saline (PBS) twice. Cells imaging was performed on a Nikon fluorescence microscopy. For the MTT assay, A549 cells were seeded in the 96-well plate with the density of 2 × 10^3 cells per well and incubated for 24 h. The culture medium was discarded and the cells were incubated in fresh culture media containing CDs with different concentrations (0−1 mg/mL) for 24 h. After removing the culture medium, 200 μL fresh culture medium (without FBS) containing MTT (20 μL, 5 mg/mL) was added and incubated for another 4 h. The formation of formazan crystals was dissolved in DMSO. The absorbance at 570 nm of the solution was recorded, and the cell viability values were calculated according to the following formula: cell viability (%) = (the absorbance of experimental group/the absorbance of control group) × 100%.[39]

2.5. Radical Scavenging Activity (RSA). The scavenging activity of CDs to DPPH free radicals was evaluated by monitoring the reduction of DPPH induced by CDs in methanol solution. In the tests, 10 μL of the CDs aqueous was added to 2 mL of DPPH (100 μM) solution. The decrease in absorption at 515 nm was measured. The RSA toward DPPH was estimated using the following equation

$$\text{inhibition (\%)} = \frac{A_c - A_s}{A_c} 100\%$$

where A_c and A_s refer to the absorbance of the DPPH at 515 nm in the absence and presence of CDs, respectively. EC_{50} (the term of the half maximal effective concentration) value was calculated to determine the 50% inhibition of the radicals. Ascorbic acid and quercetin were used as standards.

Moreover, the capability of CDs to scavenge hydroxyl radical produced by Fenton reaction was also investigated. In the test, 2 mL of $FeCl_2$ aqueous solution (1.8 mmol/mL) was mixed with 1.5 mL of salicylic acid ethanol solution (1.8 mmol/mL) and 1 mL of CDs aqueous solution (CDs concentration ranging from 0 to 1.35 mg/mL). Then 0.1 mL of H_2O_2 (100 mmol/mL) was added. Because the reaction of salicylic acid with hydroxyl radicals produces 2,3-dihydroxy benzoic and 2,5-dihydroxy benzoic which have an absorption maximum at about 510 nm,[40] by monitoring the CD-induced variation of absorption at 510 nm, the capability of CDs in scavenging hydroxyl radicals could be evaluated. The absorption spectra of the mixture solutions were acquired by a Shimadzu 1700 spectrophotometer.

3. RESULTS AND DISCUSSION

Figure 1a shows the TEM image of the as-prepared CDs. The inset histogram reveals that the CDs have a size distribution around 11 nm. Close observation of CDs by high-resolution TEM (HRTEM) observation further suggests that the CDs are in graphitic crystalline structure with the lattice spacing of about 0.35 nm (Figure 1b), corresponding to the (002) planes of graphitic carbon.[41,42] A typical X-ray diffraction (XRD) pattern in Figure 1c presents only one broad peak at about 2θ = 23.5°, which is consistent with that previously reported for CDs.[43,44] The Fourier transform infrared (FTIR) spectroscopy and X-ray photoelectron spectroscopy (XPS) were carried out

DOI: 10.1021/acsami.5b03228
ACS Appl. Mater. Interfaces 2015, 7, 17054−17060

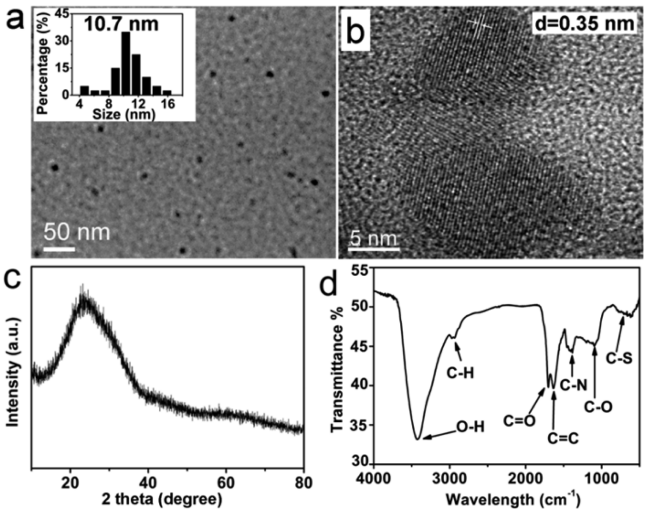

Figure 1. (a) TEM and (b) HRTEM images of the CDs. The inset shows the particle size distribution histograms of CDs. (c) XRD pattern and (d) FTIR spectrum of CDs.

to study the chemical composition and functional groups of the CDs. As depicted by the FTIR spectrum in Figure 1d, the peak at 3427 cm^{-1} is attributed to the stretching vibration of −OH; the peaks at 1720 and 1620 cm^{-1} indicate the existence of C═O and C═C, respectively; the peaks at about 2940 and 1400 cm^{-1} are assigned to the C−H and C−N stretching vibration modes, respenctively; and the absorption at 680 cm^{-1} is ascribed to the C−S group.[45]

The XPS survey spectrum in Figure 2a reveals that the CDs comprise carbon, oxygen, nitrogen and sulfur elements. The C/

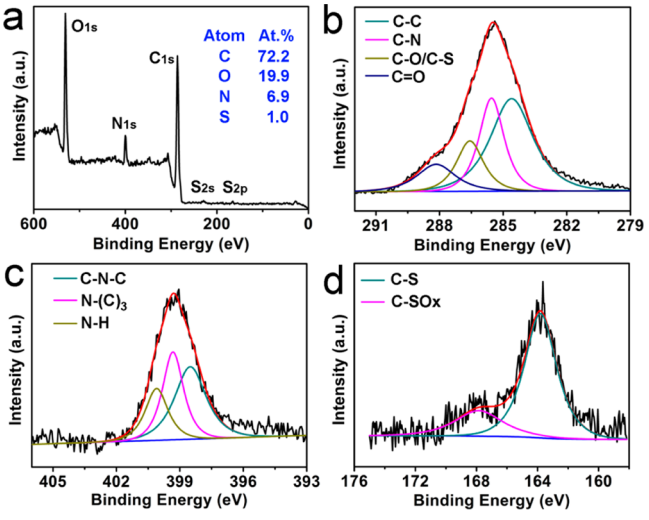

Figure 2. (a) XPS survey spectrum, and (b) C 1s, (c) N 1s, and (d) S 2p high-resolution XPS spectra of the CDs.

O/N/S atom ratio was calculated to be 72.2/19.9/6.9/1.0. The high-resolution XPS spectrum of C 1s (Figure 2b) could be resolved into four peaks with binding energies at about 284.6, 285.6, 286.6, and 288.2 eV, corresponding to C−C, C−N, C−O/C−S, and C═O, respectively. The N 1s spectrum in Figure 2c is fitted with three peaks at 398.5, 399.3, and 400.1 eV, which are ascribed to C−N−C, N−-$(C)_3$, and N−H bonds, respectively. Deconvolution of the O 1s peak gives three components at 531.3, 530.3, and 529.5 eV for the adsorbed oxygen, C−OH/C−O−C, and C═O (Figure S1), respectively; and fitting of the S 2p spectrum in Figure 2d shows two main bands at 163.8 and 167.8 eV, which are assigned to C−S and C−SO_x, respectively. Furthermore, the elemental analysis indicated the presence of C, N and S with a C/N/S atomic ratio of 88.8/9.8/1.4, which is consistent with the XPS results. The above analysis indicated that the synthesized CDs might have functional groups like −COOH, −OH, and −NH, and nitrogen and sulfur atoms were also incorporated into the CDs.

The UV−vis absorption spectrum of the CDs (Figure 3a, black line) shows a similar absorption band ranging from 200 to

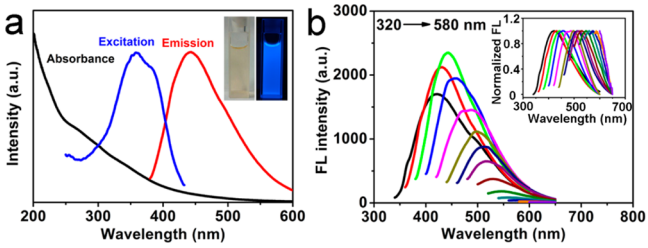

Figure 3. (a) UV−vis absorption spectrum (black line), fluorescence excitation (blue line, λ_{em} = 442 nm), and emission spectra (red line, λ_{ex} = 360 nm) of the CDs dispersed in water at room temperature. The inserts show the photograph (left) and fluorescence image of the CDs solution under UV light of 365 nm (right). (b) Fluorescence emission spectra of the CDs obtained at different excitation wavelengths with a 20 nm increment from 320 to 580 nm. Inset shows the normalized emission spectra.

600 nm with the previous report on N-doped CDs synthesized by Wu et al.[46] The CDs aqueous solution emitted strong blue light under UV irradiation of 365 nm (right inset, Figure 3a). When excited at 360 nm, the CDs showed very strong FL in the range of 380−600 nm, with the maximum located at around 442 nm (Figure 3a, red line). The fluorescent quantum yield was thus calculated to be 17.5% using quinine sulfate as a reference. The FL excitation spectrum of the CDs (FL intensity at 442 nm versus the excitation wavelength) exhibited a broad peak with the maximum at about 360 nm (Figure 3a, blue line). Figure 3b presents the FL emission spectra of the CDs obtained as the excitation wavelength increased from 320 to 580 nm by an increment of 20 nm. The spectra display a typical excitation wavelength-dependent characteristic, and the emissive wavelength is red-shifted under excitation with longer wavelengths.[47−49] The tunable emission of the CDs have been suggested to be a result of varied fluorescence characteristics of CDs of different sizes or the existence of different emissive sites on the surfaces of the CDs.[1,10,18,24] However, the exact mechanism accounting for the excitation wavelength-dependent emission remains to be established.

To investigate the applicability of CDs as a fluorescent biomarker in practical biological environment, we evaluated the fluorescent stability of CDs aqueous solution. As revealed in Figure 4a, the FL intensity of CDs solution at 442 nm fluctuated in a narrow range from 2394 to 2728 as the pH value changed from 2 to 10, and it decreased sharply in strong base aqueous solutions with the pH ranging from 11 to 13. Considering that a physiological environment has in general a pH value 7−8, which is beneficial for their bioimaging applications. Furthermore, the FL spectra of CDs were recorded in NaCl solution of different concentrations to examine the stability of CDs under high ionic strength

DOI: 10.1021/acsami.5b03228
ACS Appl. Mater. Interfaces 2015, 7, 17054−17060

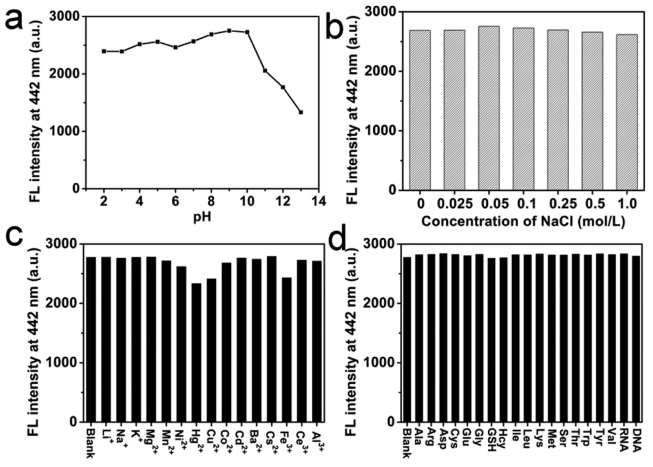

Figure 4. Effect of (a) pH value, (b) concentration of NaCl, (c) metal ions (50 μM), and (d) amino acids (50 μM), RNA and DNA (0.1 mg/mL) on the FL intensity of the CDs aqueous solution at 442 nm.

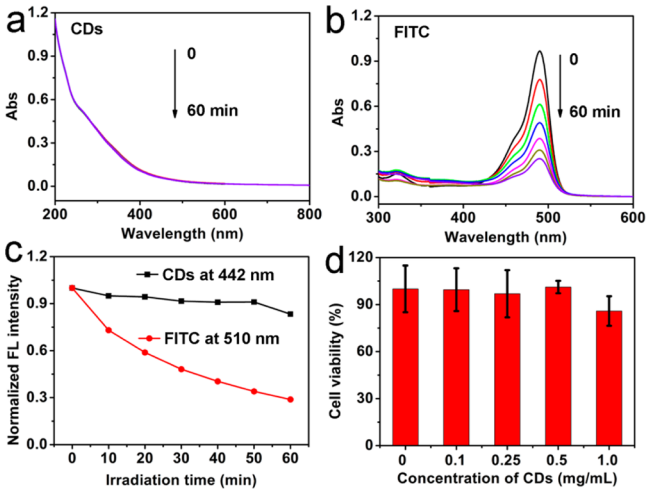

Figure 5. Absorption spectra of (a) CDs and (b) FITC (a traditional fluorescein dye, fluorescein isothiocyanate) under irradiation by a 500 W xenon lamp for different time. (c) Comparison on the photobleaching characteristics of CDs and FITC. All samples were continuously irradiated using a 500 W xenon lamp and the fluorescence intensity was normalized. (d) Cell viability values (%) estimated by MTT proliferation tests versus incubation concentrations of CDs (0, 0.1, 0.25, 0.5, 1 mg/mL) at 37 °C for 24 h.

environments. As demonstrated in Figure 4b, only a slight decrease in the FL intensities (442 nm) was observed even for a high NaCl concentration of 1 mol/L, which verifies that CDs have excellent stability at high ionic strength conditions. In addition, heavy metal ions such as Hg^{2+} and Cu^{2+} have been reported to quench the fluorescence of CDs through redox reactions or electron transfer mechanism.[50,51] Therefore, the FL characteristics of CDs solution in the presence of a variety of metal ions that may exist in living cells and some heavy metal ions were also studied, as shown in Figure 4c. The concentration of all metal ions was maintained at 50 μM. It was revealed that Hg^{2+}, Cu^{2+} and Fe^{3+} ions could induce slight variation of the FL intensity of the CDs aqueous solution (<15% quenching of the FL intensity). However, other metal ions did not show obvious interference on the FL intensity. Usually, sulfur moiety has high affinity to Hg and Cu ions, and a more significant FL quenching is expected. It has been indeed reported that the FL of the S-doped CDs could be quenched selectively and strongly by Hg^{2+} or Cu^{2+}.[52−54] However, in some other reports, the FL intensity of the S-doped CDs was less sensitive to Hg^{2+} or Cu^{2+}, but it reduced drastically upon the addition of Fe^{3+}.[55−57] It was suggested that the incorporation of S atoms in CDs could tune the electronic local density of CDs and promote the coordination interaction between Fe^{3+} ions and phenolic hydroxyl groups on the surface of S-doped CDs. The metal ion-induced FL quenching and its sensitivity to different ions are influenced by the state of sulfur impurity and the structure of CDs which are associated with the synthesis methods and the carbon sources. Moreover, the impact of biological molecules including amino acids, RNA and DNA on the FL property of CDs was further studied. As shown in Figure 4d, little changes of the FL intensity of CDs aqueous solution were observed upon their exposure to a high concentration of these interferences.

Figure 5a shows the absorption spectra of CDs under continuous irradiation by a 500 W xenon lamp for durations up to 60 min. No obvious change in the spectra could be identifies. In contrast, under the same irradiation condition, the absorbance of the commercial organic dye (FITC) was decreased to 30% (Figure 5b), suggesting a superior photostability of CDs to that of FITC. Being consistent with the outstanding photostability of CDs, the CDs aqueous solution also showed much stronger resistance to photobleaching than the FITC. As presented in Figure 5c, after irradiation for 60 min, the FL intensity of the CDs could still reserve 83%, whereas the FL intensity of FITC decreased to only 29% of its original value. Moreover, the cytotoxicity of CDs was investigated by the standard MTT assay using A549 cells as the model. The cell viabilities were examined upon exposure to the CDs of different concentrations, as depicted in Figure 5d. It reveals that the CDs exhibited extremely low cytotoxicity, i.e., viability of about 100% at a concentration of 0.5 mg/mL after 24 h incubation, and viability over 85% even at a concentration of 1 mg/mL. The above experiments indicate that the CDs synthesized in this work are featured with outstanding pH- and photostabilities, high resistance to photobleaching, inertness to interference of metal ions and biomolecular species, and excellent biocompatibility, suggesting them to be a promising candidate for bioimaging applications under physiological conditions.

Figure 6 presents the bright-field and fluorescent images of A549 cells incubated without and with CDs. The A549 cells labeled with CDs exhibited bright blue, green, and red fluorescence under ultraviolet (330−385 nm), blue (450−480 nm), and green (510−550 nm) light excitation, respectively. Close observations revealed that the CDs were distributed mainly over the cell membrane and the cytoplasmic area, and cell nucleus had only weak fluorescence. In contrast, no fluorescence signals were detected in the control cells without CDs labeling, as shown in Figure S2. This result coincides with the previous reports that CDs were able to stain both the cytoplasm and cell membrane but difficult to label the nucleus.

In this work, we also evaluated the radical scavenging activity of the N, S-*co*-doped CDs by using the DPPH as a model.[58] After accepting a hydrogen radical, DPPH was converted into stable DPPH-H complex, and the color of the solution was changed from deep violet to light yellow. The residual DPPH could be quantified by comparing absorbance at 515 nm against the blank, and the percent inhibition could be calculated. As demonstrated in Figure 7a, upon addition of 20 μg/mL CDs,

DOI: 10.1021/acsami.5b03228
ACS Appl. Mater. Interfaces 2015, 7, 17054−17060

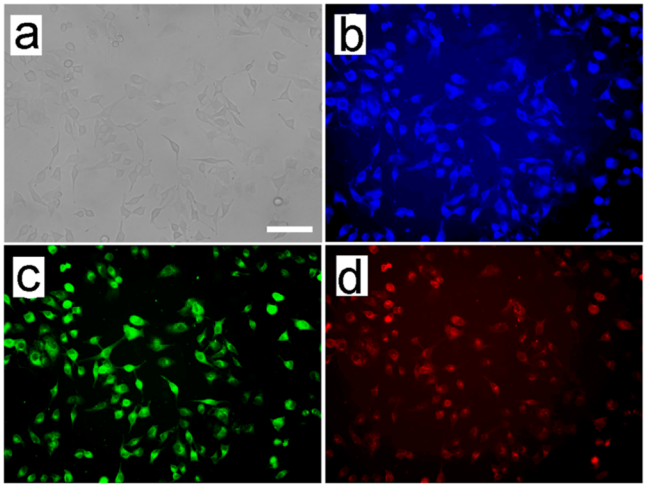

Figure 6. (a) Bright-field and (b–d) fluorescent images of A549 cells incubated with CDs. The fluorescent images were obtained at the excitation wavelengths of (b) 330–385 nm, (c) 450–480 nm, and (d) 510–550 nm. Scale bar: 50 μm.

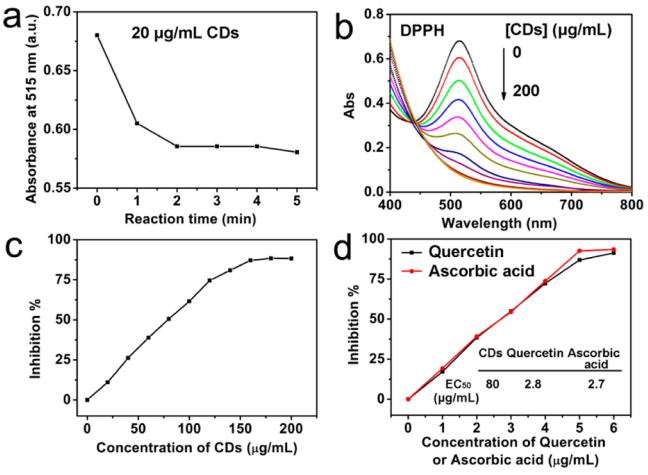

Figure 7. Scavenging of DPPH radical. (a) Scavenging of DPPH radicals as a function of time in the presence of 20 μg/mL CDs. (b) Absorbance titration spectra of DPPH upon gradual addition of CDs from 0 to 200 μg/mL. Scavenging of DPPH radicals as a function of (c) CDs concentration and (d) quercetin and ascorbic acid concentrations. The inset of d shows the EC_{50} value of CDs, quercetin, and ascorbic acid, respectively.

the absorbance of the DPPH methanol solution at 515 nm was decreased and equilibrated after 2 min which is longer than the corresponding reaction time for the commonly used free radical scavengers, ascorbic acid (30 s) and quercetin (90 s) (Figure S3). The dose-dependent scavenging of DPPH radical by CDs at concentration from 0 to 200 μg/mL was further studied, as shown in Figure 7b. Upon gradually increase of the CDs concentration, the absorbance of DPPH was decreased and saturated at [CDs] = 160 μg/mL. Further addition of CDs could not induce obvious change in the spectra. By plotting the inhibition value against the concentration of CDs, a linear relationship ($y=0.13 + 0.62x$) was obtained for a CDs concentration ranging from 0 to 120 μg/mL (Figure 7c). On the basis of that, the EC_{50} was calculated to be 80 μg/mL. As a comparison, the EC_{50} of the ascorbic acid and quercetin were about 3 μg/mL, as shown in Figure 7d. In addition, the CDs showed poor capability in scavenging hydroxyl radicals (Figure S4).

In a recent study by Das et al., CDs were prepared by microwave irradiation of date molasses, and the CDs were demonstrated to be able to scavenge the free radicals via DPPH assay. The EC_{50} value of the CDs toward DPPH was 40 μg/mL.[59] For the synthesis of CDs, the pH value of the precursor solution needed to be adjusted to ~11 by adding NaOH, and the obtained CDs-containing solution was not further purified and used directly after the pH value was tuned to ~7 by HCl. It was not verified if other molecules coexisted in the product solution and played roles in the RSA measurement. In addition, the pH dependence and photostability of the photoluminscent properties of the CDs were not shown. In comparison, though the CDs in this work showed weaker RSA capability (80 μg/mL versus 40 μg/mL of EC_{50} values toward DPPH), our CDs were prepared from garlic by hydrothermal treatment in pure water solution, and no other chemicals were required. Meanwhile, our CDs also show excellent fluorescence properties, which enable them to apply as both antioxidant and bioimaging reagents.

4. CONCLUSIONS

In summary, we have demonstrated a facile and green synthesis method to prepare fluorescent nitrogen and sulfur codoped CDs by hydrothermal reactions in pure water solution using cheap and easily obtained garlic as the reaction precursor. The CDs aqueous solution emits strong blue light under UV irradiation with a fluorescent quantum yield of 17.5%, and the emission wavelength was red-shifted under excitation with longer wavelengths. The CDs showed outstanding overall performance as compared with other fluorescent dyes, e.g., outstanding optical properties, good chemical and photochemical stability, inertness to interference of metal ions and biomolecular species, and excellent biocompatibility, which enable CDs a very desirable alternative as a probe to visualize biological systems both in vitro and in vivo. Moreover, the as-prepared CDs also exhibit favorable radical scavenging activity. The present work not only provides a new natural source to synthesize N,S-*co*-doped CDs, but also demonstrates multifunctional applications of CDs in both bioimaging and antioxidation.

■ ASSOCIATED CONTENT

Supporting Information

The Supporting Information is available free of charge on the ACS Publications website at DOI: 10.1021/acsami.5b03228.

O 1s high-resolution XPS spectra of the CDs; bright-field and fluorescent images of A549 cells without CDs; response time of ascorbic acid and quercetin toward DPPH; capability of CDs in scavenging hydroxyl radicals (PDF)

■ AUTHOR INFORMATION

Corresponding Authors

*E-mail: apwjzh@cityu.edu.hk. Tel: +(852)-34427433. Fax: +(852)-34420538.

*E-mail: xmmeng@mail.ipc.ac.cn. Tel: +86-10-82543557.

Author Contributions

The manuscript was written through contributions of all authors. All authors have given approval to the final version of the manuscript.

DOI: 10.1021/acsami.5b03228
ACS Appl. Mater. Interfaces 2015, 7, 17054–17060

Author Contributions

†S.Z. and M.L. contributed equally to this work.

Notes

The authors declare no competing financial interest.

■ ACKNOWLEDGMENTS

This work was financially supported by National Natural Science Foundation of China (51372213) and the CityU Applied Research Grant (ARG 9667089).

■ REFERENCES

(1) Baker, S. N.; Baker, G. A. Luminescent Carbon Nanodots: Emergent Nanolights. *Angew. Chem., Int. Ed.* **2010**, *49*, 6726−6744.
(2) Chen, N.; He, Y.; Su, Y. Y.; Li, X. M.; Huang, Q.; Wang, H. F.; Zhang, X. Z.; Tai, R. Z.; Fan, C. H. The Cytotoxicity of Cadmium-based Quantum Dots. *Biomaterials* **2011**, *33*, 1238−1244.
(3) Luo, Y. H.; Wu, S. B.; Wei, Y. H.; Chen, Y. C.; Tsai, M. H.; Ho, C. C.; Lin, S. Y.; Yang, C. S.; Lin, P. P. Cadmium-Based Quantum Dot Induced Autophagy Formation for Cell Survival via Oxidative Stress. *Chem. Res. Toxicol.* **2013**, *26*, 662−673.
(4) Winnik, F. M.; Maysinger, D. Quantum Dot Cytotoxicity and Ways to Reduce It. *Acc. Chem. Res.* **2013**, *46*, 672−680.
(5) Wu, C. Y.; Wang, C.; Han, T.; Zhou, X. J.; Guo, S. W.; Zhang, J. Y. Insight into the Cellular Internalization and Cytotoxicity of Graphene Quantum Dots. *Adv. Healthcare Mater.* **2013**, *2*, 1613−1619.
(6) Yang, S. T.; Cao, L.; Luo, P. J. G.; Lu, F. S.; Wang, X.; Wang, H. F.; Meziani, M. J.; Liu, Y. F.; Qi, G.; Sun, Y. P. Carbon Dots for Optical Imaging in vivo. *J. Am. Chem. Soc.* **2009**, *131*, 11308−11309.
(7) Qiao, Z. A.; Wang, Y. F.; Gao, Y.; Li, H. W.; Dai, T. Y.; Liu, Y. L.; Huo, Q. S. Commercially Activated Carbon as the Source for Producing Multicolor Photoluminescent Carbon Dots by Chemical Oxidation. *Chem. Commun.* **2010**, *46*, 8812−8814.
(8) Xu, X. Y.; Ray, R.; Gu, Y. L.; Ploehn, H. J.; Gearheart, L.; Raker, K.; Scrivens, W. A. Electrophoretic Analysis and Purification of Fluorescent Single-Walled Carbon Nanotube Fragments. *J. Am. Chem. Soc.* **2004**, *126*, 12736−12737.
(9) Shen, J. H.; Zhu, Y. H.; Yang, X. L.; Li, C. Z. Graphene Quantum Dots: Emergent Nanolights for Bioimaging, Sensors, Catalysis and Photovoltaic Devices. *Chem. Commun.* **2012**, *48*, 3686−3699.
(10) Lim, S. Y.; Shen, W.; Gao, Z. Q. Carbon Quantum Dots and Their Applications. *Chem. Soc. Rev.* **2015**, *44*, 362−381.
(11) Chen, X. X.; Jin, Q. Q.; Wu, L. Z.; Tung, C. H.; Tang, X. J. Synthesis and Unique Photoluminescence Properties of Nitrogen-Rich Quantum Dots and Their Applications. *Angew. Chem., Int. Ed.* **2014**, *53*, 12542−12547.
(12) Zhang, J.; Yuan, Y.; Liang, G. L.; Yu, S. H. Scale-Up Synthesis of Fragrant Nitrogen-Doped Carbon Dots from Bee Pollens for Bioimaging and Catalysis. *Adv. Sci.* **2015**, *2*, 1500002.
(13) Hsu, P. C.; Chen, P. C.; Ou, C. M.; Chang, H. Y.; Chang, H. T. Extremely High Inhibition Activity of Photoluminescent Carbon Nanodots toward Cancer Cells. *J. Mater. Chem. B* **2013**, *1*, 1774−1781.
(14) Lu, W. B.; Qin, X. Y.; Asiri, A. M.; Al-Youbi, A. O.; Sun, X. P. Green Synthesis of Carbon Nanodots as an Effective Fluorescent Probe for Sensitive and Selective Detection of Mercury(II) Ions. *J. Nanopart. Res.* **2013**, *15*, 1344.
(15) Yang, X. M.; Zhou, Y.; Zhu, S. S.; Luo, Y. W.; Feng, Y. J.; Dou, Y. Novel and Green Synthesis of High-Fluorescent Carbon Dots Originated from Honey for Sensing and Imaging. *Biosens. Bioelectron.* **2014**, *60*, 292−298.
(16) Liu, Y. S.; Zhao, Y. N.; Zhang, Y. Y. One-Step Green Synthesized Fluorescent Carbon Nanodots from Bamboo Leaves for Copper(II) ion Detection. *Sens. Actuators, B* **2014**, *196*, 647−652.
(17) Lu, W. B.; Qin, X. Y.; Liu, S.; Chang, G. H.; Zhang, Y. W.; Luo, Y. L.; Asiri, A. M.; Al-Youbi, A. O.; Sun, X. P. Economical, Green Synthesis of Fluorescent Carbon Nanoparticles and Their Use as Probes for Sensitive and Selective Detection of Mercury(II) Ions. *Anal. Chem.* **2012**, *84*, 5351−5357.
(18) Zhu, S. J.; Song, Y. B.; Zhao, X. H.; Shao, J. R.; Zhang, J. H.; Yang, B. The Photoluminescence Mechanism in Carbon Dots (Graphene Quantum Dots, Carbon Nanodots, and Polymer Dots): Current State and Future Perspective. *Nano Res.* **2015**, *8*, 355−381.
(19) Cao, L.; Wang, X.; Meziani, M. J.; Lu, F. S.; Wang, H. F.; Luo, P. J. G.; Lin, Y.; Harruff, B. A.; Veca, L. M.; Murray, D.; Xie, S. Y.; Sun, Y. P. Carbon Dots for Multiphoton Bioimaging. *J. Am. Chem. Soc.* **2007**, *129*, 11318−11319.
(20) Luo, P. J. G.; Sahu, S.; Yang, S. T.; Sonkar, S. K.; Wang, J. P.; Wang, H. F.; LeCroy, G. E.; Cao, L.; Sun, Y. P. Carbon "Quantum" Dots for Optical Bioimaging. *J. Mater. Chem. B* **2013**, *1*, 2116−2127.
(21) Liu, C. J.; Zhang, P.; Tian, F.; Li, W. C.; Li, F.; Liu, W. G. One-Step Synthesis of Surface Passivated Carbon Nanodots by Microwave Assisted Pyrolysis for Enhanced Multicolor Photoluminescence and Bioimaging. *J. Mater. Chem.* **2011**, *21*, 13163−13167.
(22) Yang, Y. H.; Cui, J. H.; Zheng, M. T.; Hu, C. F.; Tan, S. Z.; Xiao, Y.; Yang, Q.; Liu, Y. L. One-Step Synthesis of Amino-Functionalized Fluorescent Carbon Nanoparticles by Hydrothermal Carbonization of Chitosan. *Chem. Commun.* **2012**, *48*, 380−382.
(23) Tao, H. Q.; Yang, K.; Ma, Z.; Wan, J. M.; Zhang, Y. J.; Kang, Z. H.; Liu, Z. In vivo NIR Fluorescence Imaging, Biodistribution, and Toxicology of Photoluminescent Carbon Dots Produced from Carbon Nanotubes and Graphite. *Small* **2012**, *8*, 281−290.
(24) Li, H. T.; Kang, Z. H.; Liu, Y.; Lee, S. T. Carbon Nanodots: Synthesis, Properties and Applications. *J. Mater. Chem.* **2012**, *22*, 24230−24253.
(25) Ding, C. Q.; Zhu, A. W.; Tian, Y. Functional Surface Engineering of C-dots for Fluorescent Biosensing and in vivo Bioimaging. *Acc. Chem. Res.* **2014**, *47*, 20−30.
(26) Wang, H.; Shen, J.; Li, Y. Y.; Wei, Z. Y.; Cao, G. X.; Gai, Z.; Hong, K. L.; Banerjee, P.; Zhou, S. Q. Magnetic Iron Oxide-Fluorescent Carbon Dots Integrated Nanoparticles for Dual-Modal Imaging, Near-Infrared Light-Responsive Drug Carrier and Photothermal Therapy. *Biomater. Sci.* **2014**, *2*, 915−923.
(27) Tu, X. L.; Ma, Y. F.; Cao, Y. H.; Huang, J.; Zhang, M. X.; Zhang, Z. J. PEGylated Carbon Nanoparticles for Efficient in vitro Photothermal Cancer Therapy. *J. Mater. Chem. B* **2014**, *2*, 2184−2192.
(28) Xu, G. J.; Liu, S. J.; Niu, H.; Lv, W. P.; Wu, R. A. Functionalized Mesoporous Carbon Nanoparticles for Targeted Chemo-Photothermal Therapy of Cancer Cells Under Near-Infrared Irradiation. *RSC Adv.* **2014**, *4*, 33986−33997.
(29) Liu, J.; Liu, Y.; Liu, N. Y.; Han, Y. Z.; Zhang, X.; Huang, H.; Lifshitz, Y.; Lee, S. T.; Zhong, J.; Kang, Z. H. Metal-Free Efficient Photocatalyst for Stable Visible Water Splitting via a Two-Electron Pathway. *Science* **2015**, *347*, 970−974.
(30) Han, Y. Z.; Huang, H.; Zhang, H. C.; Liu, Y.; Han, X.; Liu, R. H.; Li, H. T.; Kang, Z. H. Carbon Quantum Dots with Photoenhanced Hydrogen-Bond Catalytic Activity in Aldol Condensations. *ACS Catal.* **2014**, *4*, 781−787.
(31) Li, H. T.; Liu, R. H.; Kong, W. Q.; Liu, J.; Liu, Y.; Zhou, L.; Zhang, X.; Lee, S. T.; Kang, Z. H. Carbon Quantum Dots with Photo-Generated Proton Property as Efficient Visible Light Controlled Acid Catalyst. *Nanoscale* **2014**, *6*, 867−873.
(32) Markovic, Z. M.; Ristic, B. Z.; Arsikin, K. M.; Klisic, D. G.; Harhaji-Trajkovic, L. M.; Todorovic-Markovic, B. M.; Kepic, D. P.; Kravic-Stevovic, T. K.; Jovanovic, S. P.; Milenkovic, M. M.; Milivojevic, D. D.; Bumbasirevic, V. Z.; Dramicanin, M. D.; Trajkovic, V. S. Graphene Quantum Dots as Autophagy-inducing Photodynamic Agents. *Biomaterials* **2012**, *33*, 7084−7092.
(33) Ristic, B. Z.; Milenkovic, M. M.; Dakic, I. R.; Todorovic-Markovic, B. M.; Milosavljevic, M. S.; Budimir, M. D.; Paunovic, V. G.; Dramicanin, M. D.; Markovic, Z. M.; Trajkovic, V. S. Photodynamic Antibacterial Effect of Graphene Quantum Dots. *Biomaterials* **2014**, *35*, 4428−4435.
(34) Juzenas, P.; Kleinauskas, A.; Luo, P. J. G.; Sun, Y. P. Photoactivatable Carbon Nanodots for Cancer Therapy. *Appl. Phys. Lett.* **2013**, *103*, 063701.
(35) Ge, J. C.; Lan, M. H.; Zhou, B. J.; Liu, W. M.; Guo, L.; Wang, H.; Jia, Q. Y.; Niu, G. L.; Huang, X.; Zhou, H. Y.; Meng, X. M.; Wang,

DOI: 10.1021/acsami.5b03228
ACS Appl. Mater. Interfaces 2015, 7, 17054−17060

P. F.; Lee, C. S.; Zhang, W. J.; Han, X. D. A Graphene Quantum Dot Photodynamic Therapy Agent with High Singlet Oxygen Generation. *Nat. Commun.* **2014**, *5*, 4596.
(36) Lan, M. H.; Zhang, J. F.; Chui, Y. S.; Wang, P. F.; Chen, X. F.; Lee, C. S.; Zhang, W. J. Carbon Nanoparticle-based Ratiometric Fluorescent Sensor for Detecting Mercury Ions in Aqueous Media and Living Cells. *ACS Appl. Mater. Interfaces* **2014**, *6*, 21270−21278.
(37) Lan, M. H.; Zhang, J. F.; Chui, Y. S.; Wang, H.; Yang, Q. D.; Zhu, X. Y.; Wei, H. X.; Liu, W. M.; Ge, J. C.; Wang, P. F.; Chen, X. F.; Lee, C. S.; Zhang, W. J. A Recyclable Carbon Nanoparticle-based Fluorescent Probe for Highly Selective and Sensitive Detection of Mercapto Biomolecules. *J. Mater. Chem. B* **2015**, *3*, 127−134.
(38) Chandra, S.; Patra, P.; Pathan, S. H.; Roy, S.; Mitra, S.; Layek, A.; Bhar, R.; Pramanik, P.; Goswami, A. Luminescent S-Doped Carbon Dots: an Emergent Architecture for Multimodal Applications. *J. Mater. Chem. B* **2013**, *1*, 2375−2382.
(39) Lan, M. H.; Zhang, J. F.; Zhu, X. Y.; Wang, P. F.; Chen, X. F.; Lee, C. S.; Zhang, W. J. Highly Stable Organic Fluorescent Nanorods for Living Cell Imaging. *Nano Res.* **2015**, *8*, 2380.
(40) Jen, J. F.; Leu, M. F.; Yang, T. C. Determination of Hydroxyl Radicals in an Advanced Oxidation Process with Salicylic Acid Trapping and Liquid Chromatography. *J. Chromatogr. A* **1998**, *796*, 283−288.
(41) Lu, J.; Yang, J. X.; Wang, J. Z.; Lim, A.; Wang, S.; Loh, K. P. One-Pot Synthesis of Fluorescent Carbon Nanoribbons, Nanoparticles, and Graphene by the Exfoliation of Graphite in Ionic Liquids. *ACS Nano* **2009**, *3*, 2367−2375.
(42) Ming, H.; Ma, Z.; Liu, Y.; Pan, K. M.; Yu, H.; Wang, F.; Kang, Z. H. Large Scale Electrochemical Synthesis of High Quality Carbon Nanodots and Their Photocatalytic Property. *Dalton Trans.* **2012**, *41*, 9526−9531.
(43) Fang, Y. X.; Guo, S. J.; Li, D.; Zhu, C. Z.; Ren, W.; Dong, S. J.; Wang, E. K. Easy Synthesis and Imaging Applications of Cross-Linked Green Fluorescent Hollow Carbon Nanoparticles. *ACS Nano* **2012**, *6*, 400−409.
(44) Zhu, C. Z.; Zhai, J. F.; Dong, S. J. Bifunctional Fluorescent Carbon Nanodots: Green Synthesis via Soy Milk and Application as Metal-Free Electrocatalysts for Oxygen Reduction. *Chem. Commun.* **2012**, *48*, 9367−9369.
(45) Yang, G. W.; Gao, G. Y.; Zhao, G. Y.; Li, H. L. Effective Adhesion of Pt Nanoparticles on Thiolated Multi-Walled Carbon Nanotubes and Their Use for Fabricating Electrocatalysts. *Carbon* **2007**, *45*, 3036−3041.
(46) Wu, Z. L.; Zhang, P.; Gao, M. X.; Liu, C. F.; Wang, W.; Leng, F.; Huang, C. Z. One-Pot Hydrothermal Synthesis of Highly Luminescent Nitrogen-Doped Amphoteric Carbon Dots for Bioimaging from Bombyx Mori Silk - Natural Proteins. *J. Mater. Chem. B* **2013**, *1*, 2868−2873.
(47) Zhang, Y. Q.; Ma, D. K.; Zhuang, Y.; Zhang, X.; Chen, W.; Hong, L. L.; Yan, Q. X.; Yu, K.; Huang, S. M. One-Pot Synthesis of N-Doped Carbon Dots with Tunable Luminescence Properties. *J. Mater. Chem.* **2012**, *22*, 16714−16718.
(48) Wang, L.; Zhou, H. S. Green Synthesis of Luminescent Nitrogen-Doped Carbon Dots from Milk and Its Imaging Application. *Anal. Chem.* **2014**, *86*, 8902−8905.
(49) Yang, Z.; Xu, M. H.; Liu, Y.; He, F. J.; Gao, F.; Su, Y. J.; Wei, H.; Zhang, Y. F. Nitrogen-Doped, Carbon-Rich, Highly Photoluminescent Carbon Dots from Ammonium Citrate. *Nanoscale* **2014**, *6*, 1890−1895.
(50) Zhou, L.; Lin, Y. H.; Huang, Z. Z.; Ren, J. S.; Qu, X. G. Carbon Nanodots as Fluorescence Probes for Rapid, Sensitive, and Label-Free Detection of Hg^{2+} and Biothiols in Complex Matrices. *Chem. Commun.* **2012**, *48*, 1147−1149.
(51) Zhu, A. W.; Ding, C. Q.; Tian, Y. A Two-Photon Ratiometric Fluorescence Probe for Cupric Ions in Live Cells and Tissues. *Sci. Rep.* **2013**, *3*, 2933.
(52) Wang, C. F.; Sun, D.; Zhou, K. L.; Zhang, H. C.; Wang, J. J. Simple and Green Synthesis of Nitrogen-, Sulfur-, and Phosphorus-co-Doped Carbon Dots with Tunable Luminescence Properties and Sensing Application. *RSC Adv.* **2014**, *4*, 54060−54065.
(53) Wang, W. P.; Lu, Y. C.; Huang, H.; Wang, A. J.; Chen, J. R.; Feng, J. J. Solvent-Free Synthesis of Sulfur- and Nitrogen-co-Doped Fluorescent Carbon Nanoparticles From Glutathione for Highly Selective and Sensitive Detection of Mercury(II) Ions. *Sens. Actuators, B* **2014**, *202*, 741−747.
(54) Lu, Y. C.; Chen, J.; Wang, A. J.; Bao, N.; Feng, J. J.; Wang, W. P.; Shao, L. X. Facile Synthesis of Oxygen and Sulfur co-Doped Graphitic Carbon Nitride Fluorescent Quantum Dots and Their Application for Mercury(II) Detection and Bioimaging. *J. Mater. Chem. C* **2015**, *3*, 73−78.
(55) Li, S. H.; Li, Y. C.; Cao, J.; Zhu, J.; Fan, L. Z.; Li, X. H. Sulfur-Doped Graphene Quantum Dots as a Novel Fluorescent Probe for Highly Selective and Sensitive Detection of Fe^{3+}. *Anal. Chem.* **2014**, *86*, 10201−10207.
(56) Ding, H.; Wei, J. S.; Xiong, H. M. Nitrogen and Sulfur co-Doped Carbon Dots with Strong Blue Luminescence. *Nanoscale* **2014**, *6*, 13817−13823.
(57) Xu, Q.; Pu, P.; Zhao, J. G.; Dong, C. B.; Gao, C.; Chen, Y. S.; Chen, J. R.; Liu, Y.; Zhou, H. J. Preparation of Highly Photoluminescent Sulfur-Doped Carbon Dots for Fe(III) Detection. *J. Mater. Chem. A* **2015**, *3*, 542−546.
(58) Katalinić, V.; Milos, M.; Modun, D.; Musić, I.; Boban, M. Antioxidant Effectiveness of Selected Wines in Comparison with (+)-Catechin. *Food Chem.* **2004**, *86*, 593−600.
(59) Das, B.; Dadhich, P.; Pal, P.; Srivas, P. K.; Bankoti, K.; Dhara, S. Carbon Nanodots from Date Molasses: New Nanolights for the in vitro Scavenging of Reactive Oxygen Species. *J. Mater. Chem. B* **2014**, *2*, 6839−6847.

DOI: 10.1021/acsami.5b03228
ACS Appl. Mater. Interfaces 2015, 7, 17054−17060